NONLINEAR DYNAMICS OF A HELICOPTER MODEL IN GROUND RESONANCE

D.M.Tang* and E.H.Dowell**
Department of Mechanical Engineering
and Material Science
Duke University, Durham, NC 27706

Abstract

An approximate theoretical method is presented which determines the limit cycle behavior of a helicopter model which has one or two nonlinear dampers. The relationship during unstable ground resonance oscillations between lagging motion of the blades and fuselage motion is discussed. An experiment has been carried out on using a helicopter scale model. The experimental results agree with those of the theoretical analysis.

Notation

H	geometrical length of the mode, see Fig.1
I	mass moment of inertia of blade relative to drag hinge
J_{fx}, J_{fz}	mass moment of inertia of fuselage about X and Z axis through A
J_{sx}, J_{sz}	mass moment of inertia of shaft about X and Z axis through A
$K_{s\ell}$	coupling spring coefficient between fuselage and shaft
$L_{v.h}$	distance from the axis of rotation center to drag hinge center
M_h	hydraulic damping moment coefficient
m_{hx}, m_{hz}	nondimensional hydraulic damping coefficients
M_d	dry friction moment coefficient
m_{dx}, m_{dz}	nondimensional dry friction damping coefficients
m_b	mass of the blade
n	number of blades
n_b	damping coefficient of blade
R	radius of the rotor blade
S	static mass moment relative to drag hinge
t	time
(A-model)	
n_0	fuselage damping coefficient
P_0	natural frequency of fuselage
ε_a	hinged mass ratio $nS^2H^2/2I(J_{sz}+J_{fz}+nm_bH^2)$
(B-model)	
n_2--n_8	damping coefficients
P_2^2--P_8^2	natural frequencies
ε_b	hinged mass ratio $nS^2H^2/2I(J_{sz}+nm_bH^2)$

(C-model)	
n_x, n_z	fuselage damping coefficients
P_x, P_z	natural frequencies of fuselage
ε_c	hinged mass ratio $nS^2H^2/2I(J_0+nm_bH^2)$
θ_{fx}, θ_{fz}	angular motion coordinate of fuselage about X and Z axis
θ_{sx}, θ_{sz}	angular motion coordinate of shaft about X and Z axis
$\theta_{fx0}, \theta_{fz0}$	angular amplitude of fuselage about X and Z axis
$\theta_{sx0}, \theta_{sz0}$	angular amplitude of shaft about X and Z axis
ψ_k	angular orientation of different rotor blades
ξ_k	angular deflection of k-th blade
ω_s	natural frequency of rotating blade relative to drag hinge
ρ_c	distance of center of gravity of the blade from drag hinge
η, ς	coordinate of the center of gravity of the blade system in fixed reference frame
ν_0	nondimensional blade parameter $\sqrt{L_{v.h}S/I}$
Ω	rotor speed

Introduction

Helicopter ground resonance is a self-excited vibration phenomenon rather than a forced vibration. The safety standards for helicopter strength require that a helicopter with an articulated rotor must have enough stable margin when it is in contact with the ground, especially, in case of rough landing. Such standards are based on linear theory, but in fact the most common design of the landing gear has nonlinear damping characteristics. How much of an effect on ground resonance will be induced? Does the nonlinear damping characteristic tend to increase stability or not? These questions are waiting for investigators to solve. The present authors [1,2] and Tongue [3] have engaged in such research. The purpose of this paper is to further study such problems.

The nonlinear damping in the landing gear of a helicopter brings into action both roll and pitch motion of the fuselage. In a series of publications [3-13] about helicopter ground resonance instability, this aspect was not taken into account by many authors. Also in the past, many investigators have used Coleman' classical multi-blade coordinate theory to simplify

---

* Visiting Scholar, Nanjing Aeronautical Institute, China.
** Dean, School of Engineering, Duke University, Durham, NC.

the study of the rotor blade dynamics. Most previous authors have considered linear dynamic models.

In the present paper, an approximate method has been used to calaulate the limit cycle behavior of a given helicopter model which has a nonlinearity in the landing gear such as a hydraulic resistance which is approximately proportional to the square of velocity or dry friction resistance. An experimental investigation has been carried out as well. The test apparatus is an improved version of Bielawa's rotor model [4]. The experimental results are in good agreement with those of the theoretical analysis.

In the present paper, we study the effect of combined roll and pitch fuselage motions, and consider the relationship between the lagging motion of the blades and the fuselage motion. Also discussed are the differences in the unstable boundary between the linear and the nonlinear model. We believe that these results will be helpful in further understanding the physical essence of helicopter ground resonance instability, and in protecting against such an instability.

Approximate method of nonlinear analysis

The analysis is based on a helicopter model with an articulated rotor. A sketch of this model is shown in Fig.1. We will assume that the blades in the plane of rotation are rigid but articulated; the spring and damping coefficients of the fuselage and the shaft are isotropic, but their mass moments of inertia are anisotropic. Nonlinear damping includes hydraulic resistance which is proportional to velocity squared and also dry friction resistance; these can be represented by $M_h |\theta| \theta$ and $M_d \text{sign}\theta$, respectively. The equations of motion for the model are six nonlinear differential equations with unknown functions η, ς, θ_{fx}, θ_{fz}, θ_{sx} and θ_{sz}. These are as follows (see Ref.[1]):

$$\ddot{\eta} + 2n_b\dot{\eta} + \omega_s^2\eta - 2\Omega(\dot{\varsigma} + n_b\varsigma) = nSH\ddot{\theta}_{sz}/2I$$

$$\ddot{\varsigma} + 2n_b\dot{\varsigma} + \omega_s^2\varsigma + 2\Omega(\dot{\eta} + n_b\eta) = -nSH\ddot{\theta}_{sx}/2I$$

$$\ddot{\theta}_{sz} + 2n_2\dot{\theta}_{sz} + (P_2^2 + P_4^2)\theta_{sz} - 2n_4\dot{\theta}_{fz}$$
$$-P_4^2\theta_{fz} = SH\ddot{\eta}/J_{sz}$$

$$\ddot{\theta}_{sx} + 2n_1\dot{\theta}_{sx} + (P_1^2 + P_3^2)\theta_{sx} - 2n_3\dot{\theta}_{fx} \tag{1}$$
$$-P_3^2\theta_{fx} = -SH\ddot{\varsigma}/J_{sx}$$

$$\ddot{\theta}_{fx} + 2n_5\dot{\theta}_{fx} + (P_5^2 + P_7^2)\theta_{fx} - 2n_7\dot{\theta}_{sx} - P_7^2\theta_{sx}$$
$$+m_{hx}\dot{\theta}_{fx}|\dot{\theta}_{fx}| + m_{dx}\text{sign}\dot{\theta}_{fx} = 0$$

$$\ddot{\theta}_{fz} + 2n_6\dot{\theta}_{fz} + (P_6^2 + P_8^2)\theta_{fz} - 2n_8\dot{\theta}_{sz} - P_8^2\theta_{sz}$$
$$+m_{hz}\dot{\theta}_{fz}|\dot{\theta}_{fz}| + m_{dz}\text{sign}\dot{\theta}_{fz} = 0$$

In order to simplify the problem, we will discuss two special cases:

1. A model with a single nonlinear damper.

We suppose that the motion in the X direction is constrained, i.e, $\theta_{sx} = \theta_{fx} = 0$, and the subscript z in θ_{sz} and θ_{fz} is thus eliminated, and define that:

$$\tilde{\theta}_s = m_{hz}\theta_s, \quad \tilde{\theta}_f = m_{hz}\theta_f$$

$$\tilde{\eta} = \eta m_{hz}SH/J_{sz}, \quad \tilde{\varsigma} = \varsigma m_{hz}SH/J_{xz}$$

Thus (1) becomes:

$$\ddot{\tilde{\eta}} + 2n_b\dot{\tilde{\eta}} + \omega_s^2\tilde{\eta} - 2\Omega(\dot{\tilde{\varsigma}} + n_b\tilde{\varsigma}) = \varepsilon_b\ddot{\tilde{\theta}}_s$$

$$\ddot{\tilde{\varsigma}} + 2n_b\dot{\tilde{\varsigma}} + \omega_s^2\tilde{\varsigma} + 2\Omega(\dot{\tilde{\eta}} + n_b\tilde{\eta}) = 0$$

$$\ddot{\tilde{\theta}}_s + 2n_2\dot{\tilde{\theta}}_s + (P_2^2 + P_4^2)\tilde{\theta}_s - 2n_4\dot{\tilde{\theta}}_f - P_4^2\tilde{\theta}_f = \ddot{\tilde{\eta}} \tag{2}$$

$$\ddot{\tilde{\theta}}_f + 2n_6\dot{\tilde{\theta}}_f + (P_6^2 + P_8^2)\tilde{\theta}_f + \dot{\tilde{\theta}}_f|\dot{\tilde{\theta}}_f| + \alpha\text{sign}\dot{\tilde{\theta}}_f$$
$$-2n_8\dot{\tilde{\theta}}_s - P_8^2\tilde{\theta}_s = 0$$

where $\quad \alpha = m_{hz}m_{dz}$

For the nonlinear terms $\dot{\theta}_f|\dot{\theta}_f|$ and $\text{sign}\dot{\theta}_f$, we apply an approximate procedure which is called quasi-linearization.

Let: $\theta_f = |\theta_f|\cos\lambda t$

Representing the above nonlinear terms by a Fourier series and retaining the first harmonic produces(see Ref.[3],[14])

$$\dot{\tilde{\theta}}_f|\dot{\tilde{\theta}}_f| = -8/3\pi*\lambda^2|\theta_{f0}|^2\sin\lambda t$$

$$\text{sign}\dot{\tilde{\theta}}_f = -4/\pi*\sin\lambda t$$

Let:

$$\tilde{\eta} = \tilde{\eta}_0 e^{i\lambda t}$$

$$\tilde{\varsigma} = \tilde{\varsigma}_0 e^{i\lambda t}$$

$$\tilde{\theta}_s = \tilde{\theta}_{s0} e^{i\lambda t}$$

Once again let:

$$\tilde{\theta}_f = \tilde{\theta}_{f0} e^{i\lambda t}$$

Substitute these expressions into Eqs.(2), and require the determinant of coefficients to be zero for nontrivial solutions. The final characteristic equations are:

real part:

$$a\tilde{\theta}_{f0}^2\lambda^8 - b\tilde{\theta}_{f0}^2\lambda^7 - c\tilde{\theta}_{f0}^2\lambda^6 + (d\tilde{\theta}_{f0}^2 + \beta b)\lambda^5 + e\tilde{\theta}_{f0}^2\lambda^4$$
$$-(f\tilde{\theta}_{f0}^2 + \beta d)\lambda^3 - g\tilde{\theta}_{f0}^2\lambda^2 + \beta f\lambda + h\tilde{\theta}_{f0}^2 = 0 \tag{3}$$

imaginary part:

$$a_1\tilde{\theta}_{f0}^2\lambda^8 + b_1\tilde{\theta}_{f0}^2\lambda^7 - (c_1\tilde{\theta}_{f0}^2 + b_0 a)\lambda^6 - d_1\tilde{\theta}_{f0}^2\lambda^5$$
$$(e_1\tilde{\theta}_{f0}^2 + \beta c_1)\lambda^4 + f_1\tilde{\theta}_{f0}^2\lambda^3 - (g_1\tilde{\theta}_{f0}^2 + \beta e_1)\lambda^2$$
$$-h_1\tilde{\theta}_{f0}^2\lambda - g_1 = 0 \tag{4}$$

The coefficients a,b,c...etc. of the above Eqs. are given in Appendix B of Ref.[1].

For the case of $K_{sf}=\infty$, $\tilde{\theta}_s=\tilde{\theta}_f=\tilde{\theta}$, i.e the shaft is connected together with fuselage, the differential equations become a simpler nonlinear mathematical model for analysing helicopter ground resonance.

$$\ddot{\tilde{\eta}}+2n_b\dot{\tilde{\eta}}+\omega_s^2\tilde{\eta}-2\Omega(\dot{\tilde{\varsigma}}+n_b\tilde{\varsigma})=\varepsilon_a\ddot{\tilde{\theta}}$$
$$\ddot{\tilde{\varsigma}}+2n_b\dot{\tilde{\varsigma}}+\omega_s^2\tilde{\varsigma}+2\Omega(\dot{\tilde{\eta}}+n_b\tilde{\eta})=0 \qquad (5)$$
$$\ddot{\tilde{\theta}}+2\tilde{n}_0\dot{\tilde{\theta}}+\dot{\tilde{\theta}}|\dot{\tilde{\theta}}|+\tilde{\theta}=\ddot{\tilde{\eta}}$$

where:

$$\tilde{n}_b=n_b/P_0,\quad \tilde{\omega}_s=\omega_s/P_0,\quad \tilde{n}_0=n_0/P_0,\quad \tilde{\Omega}=\Omega/P_0$$

For this case, the final characteristic equation is the same as in Ref[3].

Eq.(3) or (4) is eighth order in λ. Also, the $\tilde{\theta}_{f0}$ angular amplitude now appears explicitly. This means that the limit cycle amplitude of the nonlinear system is directly related to λ, the frequency of oscillation, and both must be solved for simultaneously.

The Broyden method [15] was used to solve the above simultaneous equations. Let functions $f_1(\tilde{\theta}_{f0},\lambda)$ and $f_2(\tilde{\theta}_{f0},\lambda)$ be equal to the left hand sides of Eq.(3) and Eq.(4), respectively.

$$f_1(\tilde{\theta}_{f0},\lambda)=0$$
$$f_2(\tilde{\theta}_{f0},\lambda)=0$$

2. A model with two nonlinear dampers.

We suppose:

$$K_{sf}=\infty,\quad \theta_{sx}=\theta_{fx}=\theta_x,\quad \theta_{sz}=\theta_{fz}=\theta_z$$

and define:

$$J_0=(J_x+J_z)/2,\quad \tilde{\theta}_x=\theta_x,\quad \tilde{\theta}_z=\theta_z,\quad \tilde{\eta}=\eta SH/J_0,$$
$$\tilde{\varsigma}=\varsigma SH/J_0,\quad J_x=J_{fx}+J_{sx},\quad J_z=J_{fz}+J_{sz},$$
$$\varepsilon_2=J_0/J_x,\quad \varepsilon_3=J_0/J_z$$

The general equations of motion for the model are given by Eqs.(6).

$$\ddot{\tilde{\eta}}+2n_b\dot{\tilde{\eta}}+\omega_s^2\tilde{\eta}-2\Omega(\dot{\tilde{\varsigma}}+n_b\tilde{\varsigma})=\varepsilon_c\ddot{\tilde{\theta}}_z$$
$$\ddot{\tilde{\varsigma}}+2n_b\dot{\tilde{\varsigma}}+\omega_s^2\tilde{\varsigma}+2\Omega(\dot{\tilde{\eta}}+n_b\tilde{\eta})=-\varepsilon_c\ddot{\tilde{\theta}}_x \qquad (6)$$
$$\ddot{\tilde{\theta}}_x+2n_x\dot{\tilde{\theta}}_x+P_x^2\tilde{\theta}_x+m_{hx}|\dot{\tilde{\theta}}_x|\dot{\tilde{\theta}}_x+m_{dx}\text{sign}\dot{\tilde{\theta}}_x=-\varepsilon_2\ddot{\tilde{\varsigma}}$$
$$\ddot{\tilde{\theta}}_z+2n_z\dot{\tilde{\theta}}_z+P_z^2\tilde{\theta}_z+m_{hz}|\dot{\tilde{\theta}}_z|\dot{\tilde{\theta}}_z+m_{dz}\text{sign}\dot{\tilde{\theta}}_z=\varepsilon_3\ddot{\tilde{\eta}}$$

Eqs.(6) is a set of nonlinear differetial equations for determining four unknown functions η, ς, $\tilde{\theta}_x$ and $\tilde{\theta}_z$.

Using the method of harmonic balance and retaining only the fundamental harmonic, we take

$$\tilde{\theta}_x=\tilde{\theta}_{x0}\cos\lambda t$$
$$\tilde{\theta}_z=\tilde{\theta}_{zc}\cos\lambda t+\tilde{\theta}_{zs}\sin\lambda t=\tilde{\theta}_{z0}\cos(\lambda t-\varphi_z)$$
$$\tilde{\eta}=\tilde{\eta}_c\cos\lambda t+\tilde{\eta}_s\sin\lambda t=\tilde{\eta}_0\cos(\lambda t-\varphi_\eta) \qquad (7)$$
$$\tilde{\varsigma}=\tilde{\varsigma}_c\cos\lambda t+\tilde{\varsigma}_s\sin\lambda t=\tilde{\varsigma}_0\cos(\lambda t-\varphi_\varsigma)$$

Here φ_z, φ_η, φ_ς are respectively the phase difference of $\tilde{\theta}_z$, $\tilde{\eta}$ and $\tilde{\varsigma}$ with respect to $\tilde{\theta}_x$

Now we consider the term $\text{sign}\dot{\tilde{\theta}}_z$ and $\dot{\tilde{\theta}}_z|\dot{\tilde{\theta}}_z|$. As was mentioned previously [2], we can obtain the following approximate result:

For λ, $\tilde{\theta}_{z0}>0$

$$\text{sign}\dot{\tilde{\theta}}_z\cong\frac{4}{\pi\tilde{\theta}_{z0}}(\tilde{\theta}_{zs}\cos\lambda t-\tilde{\theta}_{zc}\sin\lambda t)$$

$$|\dot{\tilde{\theta}}_z|\dot{\tilde{\theta}}_z=\frac{-8\lambda^2}{3\pi}\tilde{\theta}_{z0}(\tilde{\theta}_{zc}\sin\lambda t-\tilde{\theta}_{zs}\cos\lambda t)$$

Inserting Eq.(7) into Eq.(6) we obtain a system of eight simultaneous nonlinear algebraic equations for determining the quantities, $\tilde{\eta}_c,\tilde{\eta}_s,\tilde{\varsigma}_c,\tilde{\varsigma}_s,\tilde{\theta}_{x0},\tilde{\theta}_{zc},\tilde{\theta}_{zs}$ and λ.

By elimination of the first four unknowns, the equations can be rewritten more compactly as a matrix equation with four unknowns, $\tilde{\theta}_{x0},\tilde{\theta}_{zc},\tilde{\theta}_{zs},\lambda$.

Let:

$$\{F\}\equiv\{U\}+[V]^{-1}\{\tilde{\theta}\}=\{0\} \qquad (8)$$

where

$$[V]=\begin{bmatrix}-a & -b & c & d \\ b & -a & -d & c \\ c & d & a & b \\ -d & c & -b & a\end{bmatrix}\qquad\{\tilde{\theta}\}=\begin{Bmatrix}\tilde{\theta}_{zc}\\ \tilde{\theta}_{zs}\\ \tilde{\theta}_{x0}\\ 0\end{Bmatrix}$$

$$\{U\}=\begin{Bmatrix}(P_z^2/\lambda^2-1)\tilde{\theta}_{zc}/\varepsilon_3+2n_z\tilde{\theta}_{zs}/\lambda\varepsilon_3+\\ 8m_{hz}\tilde{\theta}_{z0}\tilde{\theta}_{zs}/3\pi\varepsilon_3+4m_{dz}\tilde{\theta}_{zs}/\pi\lambda^2\tilde{\theta}_{z0}\varepsilon_3\\ (P_z^2/\lambda^2-1)\tilde{\theta}_{zs}/\varepsilon_3-2n_z\tilde{\theta}_{zc}/\lambda\varepsilon_3-\\ 8m_{hz}\tilde{\theta}_{z0}\tilde{\theta}_{zc}/3\pi\varepsilon_3-4m_{dz}\tilde{\theta}_{zc}/\pi\lambda^2\tilde{\theta}_{z0}\varepsilon_3\\ (1-P_x^2/\lambda^2)\tilde{\theta}_{x0}/\varepsilon_2\\ 2n_x\tilde{\theta}_{x0}/\lambda\varepsilon_2+4m_{dx}/\pi\varepsilon_2\lambda^2+8m_{hx}\tilde{\theta}_{x0}^2/3\pi\varepsilon_2\end{Bmatrix}$$

$$a = (\omega_s^2/\lambda^2 - 1)/\varepsilon_1$$
$$b = 2n_b/\varepsilon_1\lambda$$
$$c = 2\Omega n_b/\varepsilon_1\lambda^2$$
$$d = 2\Omega/\varepsilon_1\lambda$$

$$\{F\} = \begin{Bmatrix} f_1 \\ f_2 \\ f_3 \\ f_4 \end{Bmatrix}$$

In order to solve Eq.(8), the elements of {F} must be zero. Here we also apply Broyden's method to solve the above equation.

Experimental Investigation

1. Experimental equipment

An overall view of the test model and recording equipment used in this study is shown in Figs.2 and 3. The details of the various components of the model appear in Ref.[1] and [2]. The A-model has only one degree of freedom for fuselage motion. The B-model has two degrees of freedom for shaft and fuselage motion. The C-model has two degrees of freedom for the roll and the pitch motion of the fuselage. The characteristic curves of the hydraulic and dry friction damping are shown in Fig.4(a) and (b). The method of determining these parameters is described in Ref.[1].

2. Measurement system

The X and Z angular displacements and velocities of the fuselage and the shaft are obtained by RVDT, R30D, velocity transducers located near the dry friction dampers, and a LVDT located near the gimbal support assembly. The output voltage of the transformers and velocity transducers is proportional to angular displacement and velocity of the roll and the pitch of the fuselage and the shaft. The output from the transformers are amplified and recorded on a multiple channel tape recorder, HP3968A.

In order to obtain a one per revolution signal and the lagging motion of the individual blades during rotation of the blades, we mount a 13-ch brush and slip ring assembly on the shaft between the electric motor and hub, see Fig.5. One of these slip rings is not a closed ring. It gives an impulsive signal once per revolution, so a very accurate measurement of rotor speed can be provided. Three angular transducers, R30A, are mounted on the drag hinges. The signals for lagging motion of each blade were amplified and recorded through brush and slip ring assemblies. The 8 channel signals were recorded simultaneously on a tape recorder, and further analysed by a Frequency Spectral Analyzer, HP3582A. Finally, the phase plane plots and frequency spectral plots were plotted by a X-Y recorder.

The stability test needs an initial disturbance, so two electro-magnets were mounted on the test equipment. Those are used to generate a disturbance in the direction of roll or pitch of the fuselage.

The device for angular amplitude calibration is shown in Fig.6. An electric motor with stepless variable speed provides a vibration source, and drives a cam which can generate a sine wave, such that the relationship between output voltage from the transducers and the actual angle can be determined.

3. Frequency response test

The purpose of the frequency response test is to determine the natural frequencies of the system, and to provide an independent check on the system parameters. Before the test, the drag hinges are fixed, and a known block mass (3 oz) is put on a drag hinge. A centrifugal force caused by the bias mass will excite the system, and the frequency response versus rotor speed can be found.

4. Stability test

Testing the model for self-excited instability regions was accomplished by slowly varying the rotor speed until instability was observed in response to an initial disturbance.

Results and Discussion

Fig.7 shows the limit cycle behavior when only the hydraulic nonlinearity is present in the A-model. The figure shows that the maximum limit cycle amplitude occurs near the critical rotor speed of the linear system, and that the dominant response occurs in the region, $(1.7-2.0)*\Omega$. Furthermore, there is an abrupt change in response from $(1.9-1.95)*\Omega$ in Fig.7. This means that the amplitude response is very sensitive to small changes in rotor speed in this range of rotor speed.

Fig.8 shows the limit cycle behavior with both hydraulic and dry friction nonlinearities. The curve has a shape similar to that of Fig.7, but the response amplitude is smaller than that in Fig.7. Physically the action of dry friction is to increase the equivalent viscous damping in the landing gear. The instability region becomes narrower, and the response amplitude reduces.

Fig.9 shows the limit cycle behavior of the B-model. There are two instability regions in the figure. The first one is dominated by the shaft motion. Because the effect of nonlinear damping of the fuselage on the shaft is weak, the shaft has a large limit cycle amplitude (for

some range of Ω beyond the measurable angle). In contrast with the first region, in the second instability region there is not a large limit cycle amplitude because of the direct effects of nonlinear damping of the fuselage on the fuselage motion.

As far as the C-model is concerned, Fig.10 shows the results of frequency spectral analysis of the fuselage motion at a rotor speed of 1.2(HZ). The mode shape of the unstable motion is dominated by roll of the fuselage, and the oscillation frequency is equal to the roll natural frequency of the fuselage. Simultaneously, there is a small limit cycle amplitude in the pitch motion; its oscillation frequency is not equal to the pitch natural frequency, but is equal to the roll natural frequency. The phase angle between roll and pitch is equal to $51°$, corresponding to a frequency of 0.84(HZ). The phase curve in the vicinity of 0.84(HZ) is almost parallel to the frequency axis, and the phase angle is quite insensitive to frequency.

Fig.11-12 show theoretical and experimental results of the limit cycle amplitude and phase angle behavior. A reasonable experimental verification of the theory is achieved. Because of the experimental complexity and calculation approximation, the quantitative accuracy of the verification is not very high. However, the general features of the experimental results are well predicted by the theory. For reference, in Fig.13 the stability boundary results from linear theory are shown and compared to experimental data obtained with the nonlinear dampers removed. The agreement between theory and experiment in this case is good.

Fig.14 shows a phase plane plot which is directly plotted by a X-Y recorder. The measurement point of displacement and velocity is located at the same position. Their phase difference approximates to $90°$, the pattern displays an ellipse approximately, and the higher order harmonic components are included in the ellipse curve. From this pattern, we also can see the transient process leading to the steady state limit cycle amplitude. Different disturbances have different unstable processes. In this case the roll oscillation of the fuselage tends to a limit after about 7 pseudo cycles, and the transient process includes more higher order harmonic components.

Fig.15 shows the results of a frequency spectral analysis of the lagging motion of the individual blades at a rotor speed of 2.04(HZ). It is found that in the instability region the individual blades have an identical oscillation frequency, p, which is equal to the difference between the rotor speed and the oscillation frequency, λ, of the fuselage. This result is in agreement with conclusion which is derived by classical linear theory. However, the individual blades have different amplitudes and phase angles due to the actual small different blade damping characteristics.

The equation of motion of the k-th blade can be written as follows:

$$\ddot{\zeta}_k + 2n_b\dot{\zeta}_k + \omega_s^2\zeta_k = \frac{\nu_b}{L_{v.h}}(\ddot{X}\sin\psi_k - \ddot{Z}\cos\psi_k)$$

The periodic term in the above equation can be removed by using the Coleman co-ordinates.

$$\eta = \sum_{k=1}^{n}\zeta_k\sin\psi_k$$
$$\zeta = \sum_{k=1}^{n}\zeta_k\cos\psi_k$$

If it is expected that η and ζ are well represented by a fundamental harmonic with oscillation frequency, λ, then ζ_k may be defined as:

$$\zeta_k = \zeta_0\cos(Pt + 2\pi k/n)$$

i.e the following conditions must be satisfied:

* $p = \Omega - \lambda$
* the amplitudes of the individual blades are identical.
* the phase angle of the k-th blade is equal to $2k\pi/n$.

In the present experiment, only the first condition is satisfied. The modest violations of the latter two conditions are the main reasons for the error between theoretical and experimental results.

In order to provide a better physical understanding of the unstable motion, we discuss the relationship between motion of the hub center and the center of gravity (C.G) of the blades. In the fixed coordinate system X0Z, the motion of the common center of gravity of the blade system is expressed by

$$X_c = X - \frac{\rho_c}{n}\sum_{k=1}^{n}\zeta_k\sin\psi_k$$
$$Z_c = Z + \frac{\rho_c}{n}\sum_{k=1}^{n}\zeta_k\cos\psi_k$$
$$X = H\sum_{i=1}^{m}\theta_{x0i}\cos\lambda_i t$$
$$Z = H\sum_{i=1}^{m}\theta_{z0i}\cos(\lambda_i t - \varphi_{zi})$$

Fig.16 shows the time history of η and ζ. The test curves include components with frequency $(2\Omega - \lambda)$, and λ, in addition, a $\cos\lambda t$ component. This also can be clearly found from Fig.17. The motion locus of the C.G of the blades is not exactly an ellipse, but a somewhat more complicated curve. The starting point at t=0 does not

coincide with the end point at t=2(sec.), however over a much longer time interval, the motion does appear periodic. The phase angle between hub center and C.G of blades is equal to $46°$ from calculation, and $15°$ from test. The phase angle depends upon the dampings of the fuselage and blades, as well as rotor speed.

Fig.18 shows the theoretical and experimental results for a rotor speed of 1.2(HZ). The test curves are approximately cosine waves. The motion locus of the C.G of the blades approximates to an ellipse, and excellent agreement of calculation with test is achieved for the motion locus of the hub center. As compared with Fig.17 and 18, we find that the difference between theory and experiment for the hub center motion mainly comes from the variation of blade motion from one blade to the next.

Fig.19 shows the test results for a rotor speed of 1.96(HZ). All higher order harmonic components are included in the motion of the fuselage and blades. Their motion loci have quite complex shapes, but they always tend to a limit amplitude.

Conclusions

A number of conclusions may be reached.

1. Unstable motion of a helicopter in ground resonance can occur only when the rotor speed is within a certain region, and at the same time a initial disturbance acts on it. This conclusion is suitable for both linear and nonlinear systems.

2. During unstable motion the oscillation frequency is equal to the natural frequency of the linear system, or approximately the natural frequency for a nonlinear system.

3. The nonlinear dynamic rotor system with multiple nonlinear dampers has more complex motions than the system with a single nonlinear damper. The coupled motion of roll and pitch of the fuselage is due to blade lagging motion. This coupling motion is important in understanding ground resonance of an actual helicopter.

4. The agreement of theory with the experimental results verifies that the analytical method which is described in this paper is useful and reliable.

5. The different characteristics of individual lag blade dampers will lead to different limit cycle behavior.

6. The results show that a landing gear with hydraulic nonlinear damping characteristics and dry friction damping may be advantageous for protecting against ground resonance instability. It is unlikely, perhaps, that a helicopter resigner would rely on a nonlinear damper for primary protection against ground resonance. However, such a damper may be useful as a failsafe device to ensure a benign failure mode should a primary linear damper become inoperable or prove inadequate under some operating conditions.

7. It is expected that the design and operation of blade dampers will also be very important for avoiding ground resonance. This is a logical topic for future study.

References

1. Tang D.M and Dowell E.H, "Nonlinear Dynamics of a Helicopter Model in Ground Resonance. Part 1: Analysis and Experiment on a Helicopter Model with Single Nonlinear Damper and Fuselage Motion", Duke University, Engineering School Report, March 1984.

2. Tang D.M and Dowell E.H, "Nonlinear Dynamics of a Helicopter Model in Ground Resonance. Part 2: Analysis and Experiment on a Helicopter Model with Multiple Nonlinear Dampers and Roll and Pitch Fuselage Motion", Duke University, Engineering School Report, May 1984.

3. Tongue,Benson H.,"Limit Cycle Oscillations of a Nonlinear Rotorcraft Model", AIAA Journal, to be published.

4. Bielawa,Richard L.,"An Experimental and Analytical Study of the Mechanical Instability of Rotor on Multiple-Degree-of Freedom Supports", Princeton University, M.S.E. Thesis, June 1962.

5. Coleman, R.P. and Feingold, A.M., "Theory of Self Excited Mechanical Oscillations of Helicopter Rotors with Hinged Blades", NACA Report 1351, Feb.1957.
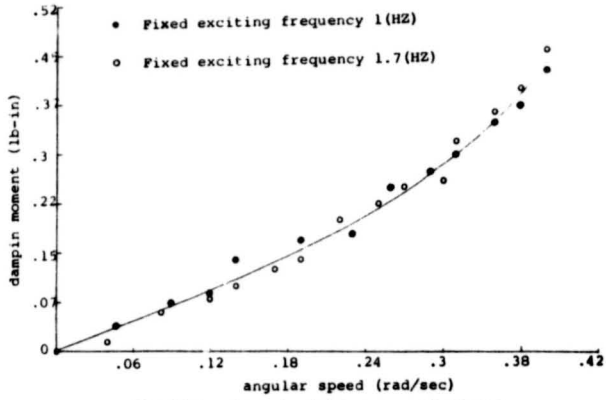
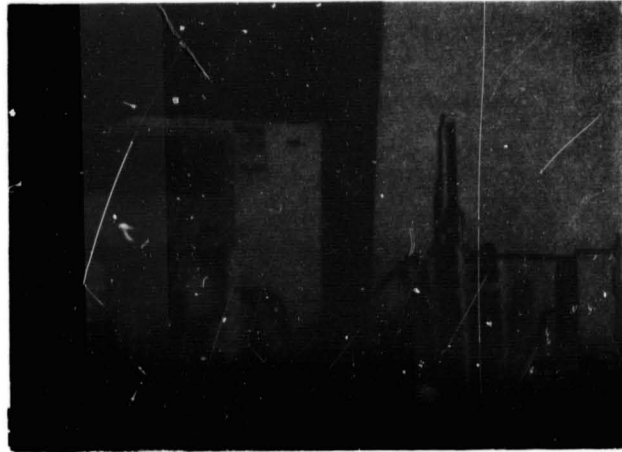6. Brook,G.W.,"The Mechanical Instability and Forced Response of Rotors on Multiple Degree of Freedom Supports", Ph.D Thesis, Princeton University, Department of Aeronautical Engineering, Oct.1961.

7. Hohenemser,K.H. and Yin,S.K.,"Some Applications of the Method of Multi-Blade Coordinates", Journal of the American Helicopter Society, Vol.7,No.3 July 1972.

8. Price,H.L.,"The Avoidance of Ground Resonance", Aircraft Engineering, Vol.17, No.376, June 1960.

9. Done,G.T.S."A Simplified Approach to Helicopter Ground Resonance", ARC 33254, 1971.

10. Dowell,Earl H.,et al., A Modern Course in Aeroelasticity, Sijithoff and Noordhoff, 1980.

11. Mil,M.L. et al.,"Helicopter-- Calculation and Design, Vol. II, Vibration and Dynamic Stability", NASA TT F-519,May 1968.

12. Howarth,R.M., and Jones,C.H.,"Ground Resonance of Helicopter", The Journal of Helicopter Association of G.B, Vol.7, No.4, April 1954.

13. Johnson,W., Helicopter Theory, Princeton University Press,Princeton,N.J., 1980.

14. Dowell, Earl H.,"The Behavior of A Linear Damped Modal System with A Nonlinear Spring-Mass-Dry Friction Damper Attached", Journal of Sound and Vibration, 89(1),1983.

15. Broyden, C.G.,"A New Method of Solving Nonlinear Simultaneous Equations", Computer Journal, Vol.12, No 1, 1969.

Fig.1

Fig.2. test model

Fig.3. test equipment

Fig.4(a). characteristic curve of damper

Fig.6. calibration device of angular amplitude
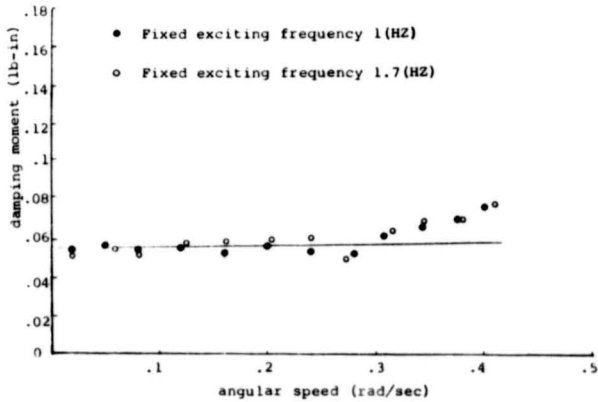
Fig.4(b). characteristic curve of damper
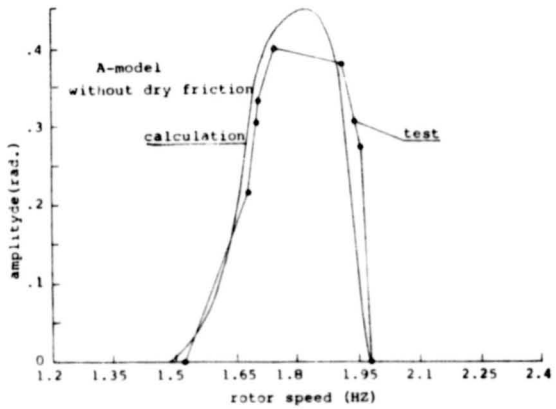
Fig.7. limit cycle behavior
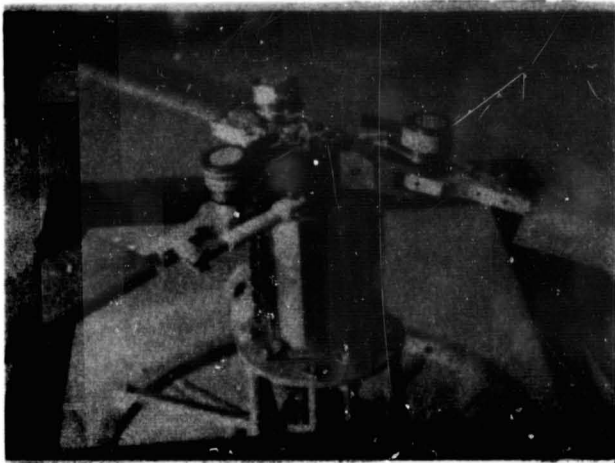
Fig.5. measurement system of rotor blade
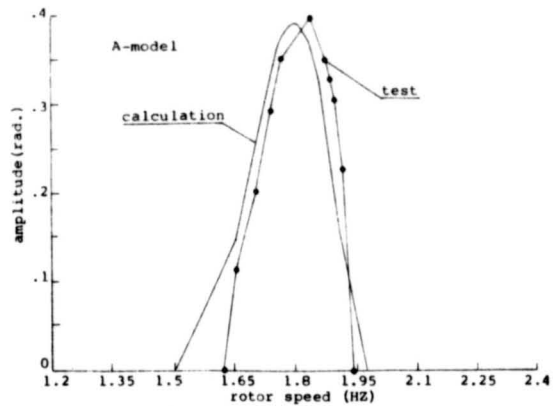
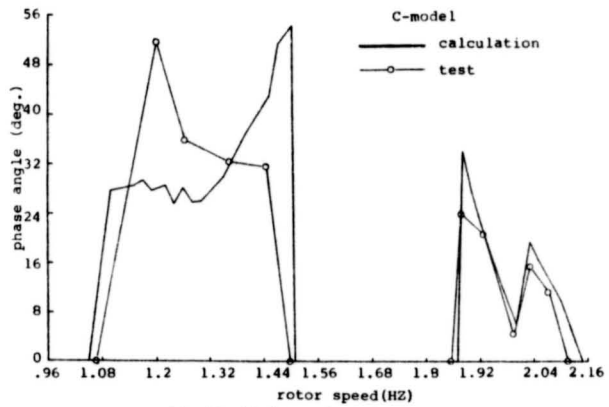Fig.8. limit cycle behavior
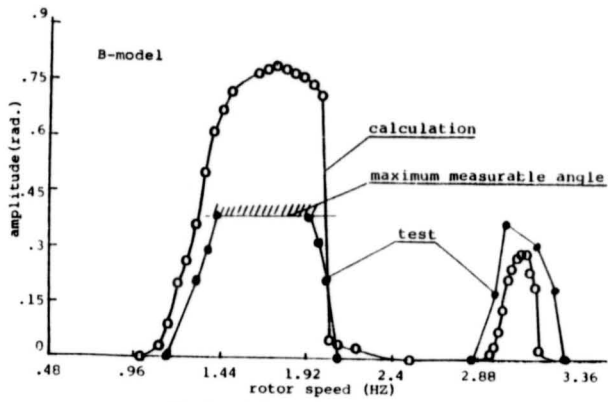
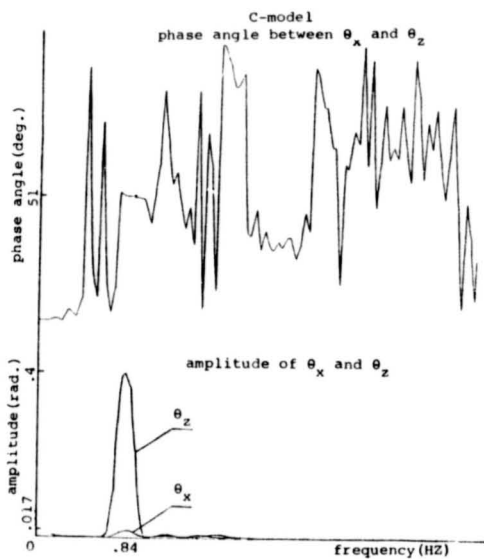Fig.9. limit cycle behavior

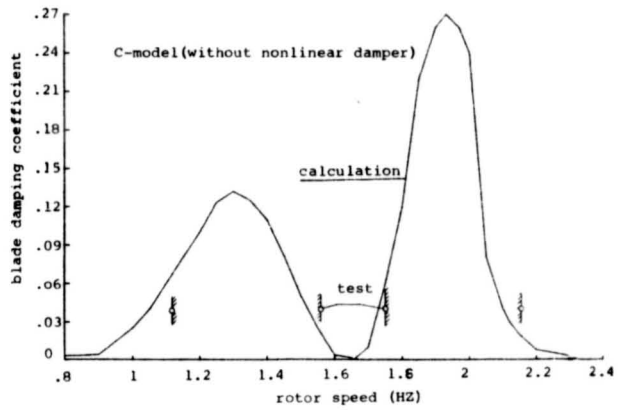Fig.12. limit cycle behavior

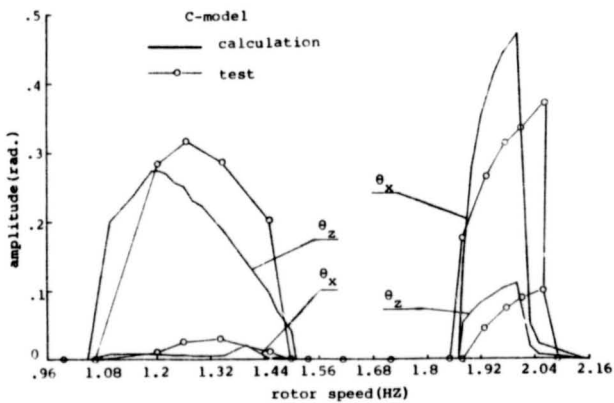Fig.10. frequency spectral analysis

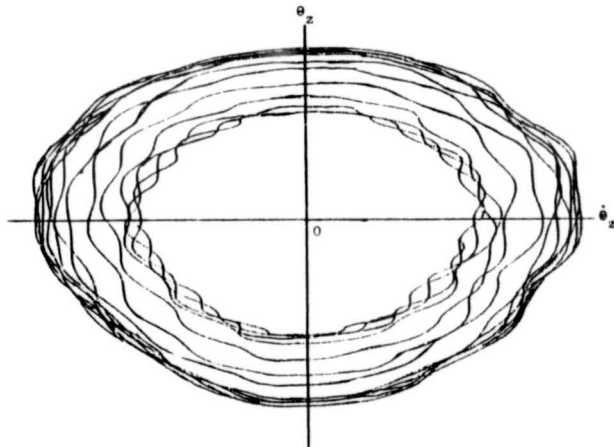
Fig.13. instability region

Fig.11. limit cycle behavior

Fig.14. phase plane plot

phase angle between ζ_1 and ζ_3

amplitude of ζ_1 and ζ_3
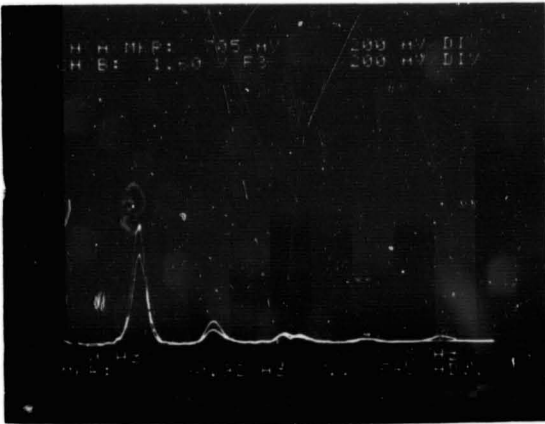
Fig.15. frequency spectral analysis
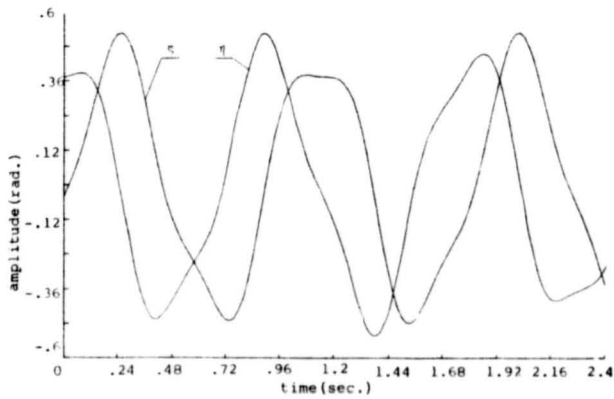
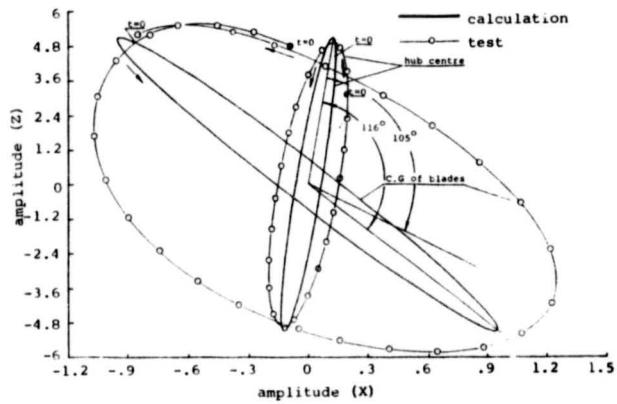Fig.17. motion locus

Fig.18. motion locus
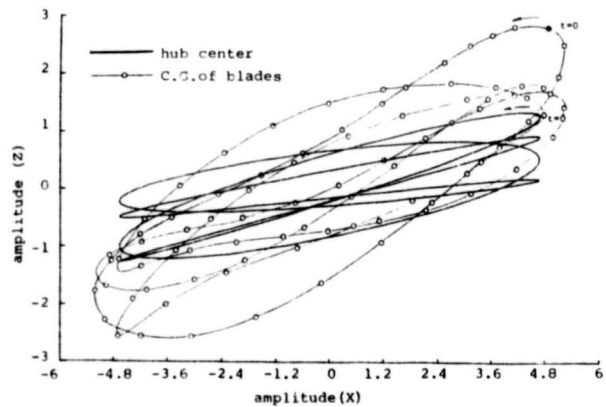

Fig.16. time history

Fig.19. motion locus

DISCUSSION
Paper No. 4

NONLINEAR DYNAMICS OF A HELICOPTER MODEL IN GROUND RESONANCE
D. M. Tang
and
E. H. Dowell

<u>Jerry Miao, Sikorsky Aircraft</u>: I would like to make a comment. Earlier Jing Yen said that we may not be able to analyze ground resonance, but apparently from this paper we can see with a nonlinear damper we can even calculate the amplitude of the oscillation. Therefore, if you only know what numbers to put into the analysis you will be able to calculate it. Thank you.